The Effect of Water Hammer upon Pipes at Suddenly Closed Valve

Mahned Sahib
College of Engineering
University of Thi-Qar

Hussam Ali Khalaf
Marshes Research Centre
University of Thi-Qar

Abstract

The paper aims at a detailed description of the water hammer due to a sudden valve closure. The transients of flow are computed by characteristic method and compared with many studies, experimental results, mathematical models and numerical simulations of other authors, as shown excellent agreement can be observed.

الملخّص

يُهدَفُ هذا البحث الى وصفَ مطرقةِ الماءَ الناتجة بسبب إغلاق صمامِ مفاجئ. إنّ تدفقِ الجريان حسب بالطريقةِ المميزةِ وتمت المقارنة النتائج المستحصلة مع الدِراساتِ، والنَتائجِ العمليةِ ة، والنمَاذج الرياضية والمحاكاةَ العدديةَ مِنْ المُؤلفين الآخرينِ، وسمكن ملاحظ التوافق الممتاز لهذه النتائجَ.

1. Background

The water hammer phenomenon is usually explain by considering an ideal reservoir-pipe-valve system in which a steady flow with velocity V_0 is stopped by an instantaneous valve closure (see Fig. 1). The valve closure generates a pressure wave which travels at the wave speed or celerity, *a*, towards the reservoir at distance, *L*. The amplitude, *P*, of the pressure wave is given by the Joukowsky formula

$$\text{..... (1)}\quad P = \rho a V_{\circ}$$

where ρ is the mass density of the fluid. The traveling pressure wave reflects at the reservoir and returns at the valve at time 2*L*/*a*. Finally, a standing wave occurs in the pipe. In fact, water hammer is nothing more than the free vibration of the liquid column. The natural frequency of the vibration is *a*/(4*L*) for the open-closed system of Fig. 1, Bergant, A. and Tijsseling, A. (2001).

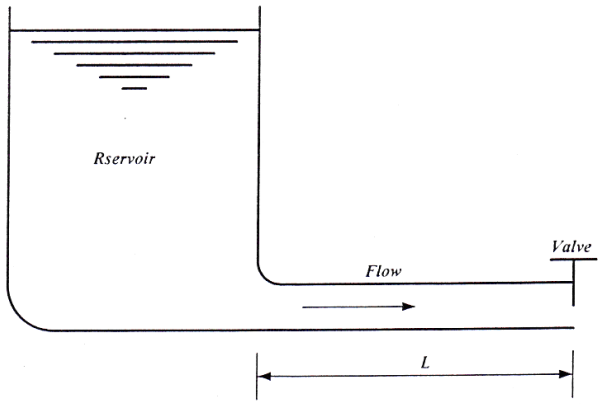

Fig.1 Reservoir-pipe-valve system

2. Basic Water Hammer

The pressure waves in the ideal system of Fig. 1 are plane waves that obey the standard wave equation

$$\ldots (2)\ \frac{\partial^2 P}{\partial t^2} - a^2 \frac{\partial^2 P}{\partial x^2} = 0$$

with *t* =time, *x*=axial distance, and the wave speed given by the Korteweg formula

$$\ldots (3)\ a = \sqrt{\frac{K}{\rho}} \sqrt{\frac{1}{1+\psi \frac{DK}{eE}}}$$

where *K* = bulk modulus of elasticity of the fluid, *E* = Young's modulus of elasticity of the pipe material, *D* = pipe diameter, *e* = pipe thickness and ψ = 1. The coefficient ψ accounts for the support conditions of the pipe and it may take values between 0.75 and 1. Eq (2) has exact solutions according to D'Alembert. The pressure histories at valve and midpoint in Fig. 2 are the exact solutions for water hammer in an ideal reservoir-pipe-valve system, Bergant, A., et al., (2005).

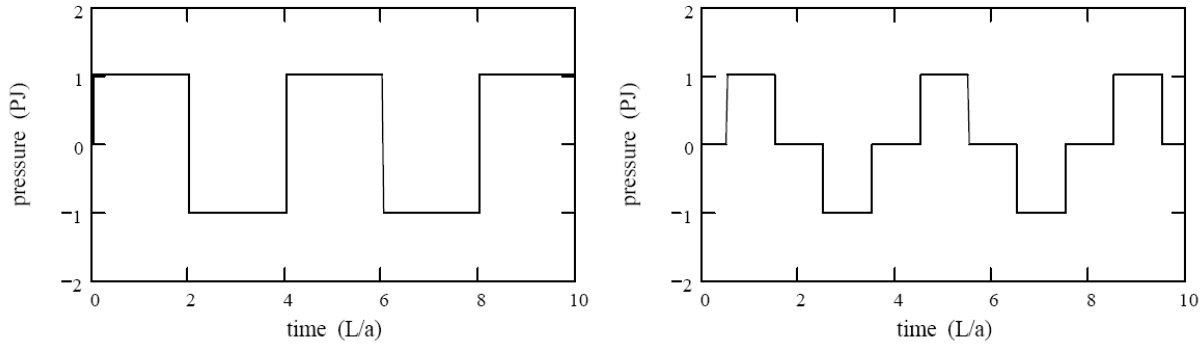

Fig. 2 Basic water hammer in reservoir-pipe-valve system.
Left: pressure at valve. Right: pressure at midpoint.

3. Classic Water Hammer

The pressure variations in Fig. 2 repeat forever; however, in reality, the pressure variations will die out because of friction and damping mechanisms. The classic theory of water hammer takes into account the effect of skin (fluid-wall) friction. In fact, it describes the transient free vibration of a liquid column. Pressure, P, and average velocity, V, obey the equations for conservation of mass and momentum, Vuuren, S.(2002):

$$\ldots(4)\ \frac{1}{\rho}\frac{dP}{dt}+a^2\frac{\partial V}{\partial x}=0$$

$$\ldots(5)\ \frac{dV}{dt}+\frac{1}{\rho}\frac{\partial P}{\partial x}+g\sin\theta+\frac{fV|V|}{2D}=0$$

4. Characteristic Method

The characteristic method provides a popular technique for solving transient flow equations and has many advantages, Vuuren, S.(2002):

- **Stability criteria are firmly established.**
- **Boundary conditions are programmable.**
- **Minor loss terms may be retained if desired.**
- **Extremely complex systems may be handled.**
- **It is the most accurate of any of the finite difference methods.**
- **It allows detailed analysis of complex systems.**

The two equations (4) and (5) may be replaced by some their linear combination.
Using λ as a linear scale factor:

$$\ldots(6)\ \lambda\left(\frac{\partial V}{\partial t}+\frac{1}{\rho}\frac{\partial P}{\partial x}+g\sin\theta+\frac{fV|V|}{2D}\right)+\left(\frac{1}{\rho}\frac{\partial P}{\partial t}+a^2\frac{\partial V}{\partial x}\right)=0$$

Regrouping terms:

$$\ldots(7)\left(\lambda\frac{\partial V}{\partial t}+a^2\frac{\partial V}{\partial x}\right)+\left(\frac{1}{\rho}\frac{\partial P}{\partial t}+\frac{\lambda}{\rho}\frac{\partial P}{\partial x}\right)+\lambda g\sin\theta+\lambda\frac{fV|V|}{2D}=0$$

Note that: $\frac{dV}{dt}=\frac{\partial V}{\partial t}+\frac{\partial V}{\partial x}\frac{dx}{dt}$

Multiplying by (λ) gives: $\lambda\frac{dV}{dt}=\lambda\frac{\partial V}{\partial t}+\lambda\frac{\partial V}{\partial x}\frac{dx}{dt}$

if $\lambda\frac{\partial V}{\partial t}+a^2\frac{\partial V}{\partial x}$ **is to be replaced by** $\lambda\frac{dV}{dt}$ **then** $\lambda\frac{dx}{dt}=a^2$

and as $\frac{dP}{dt}=\frac{\partial P}{\partial t}+\frac{\partial P}{\partial x}\frac{dx}{dt}$

Multiplying by (λ) gives: $\lambda \frac{dP}{dt} = \lambda \frac{\partial P}{\partial t} + \lambda \frac{\partial P}{\partial x}\frac{dx}{dt}$

if $\frac{1}{\rho}\frac{\partial P}{\partial t} + \frac{\lambda}{\rho}\frac{\partial P}{\partial x}$ **is to be replaced by** $\frac{1}{\rho}\frac{dP}{dt}$ **then** $\frac{\lambda}{\rho} = \frac{1}{\rho}\frac{dx}{dt}$

Equating the expression for (*ds/dt*) in each case, the following is obtained:

$$\ldots (8)\ \frac{a^2}{\lambda} = \lambda \quad \text{or} \quad a^2 = \lambda^2$$

So both equations are satisfied if $\lambda = \pm a$ **. Arbitrarily picking** $\lambda = +a$ **permits to rewrite equation (7) as :**

$$\ldots (9)\ a\frac{dV}{dt} + \frac{1}{\rho}\frac{dP}{dt} + ag\sin\theta + a\frac{f}{2D}V|V| = 0$$

Dividing through the wave speed, (a), gives:

$$\ldots (10)\ \frac{dV}{dt} + \frac{1}{a\rho}\frac{dP}{dt} + g\sin\theta + \frac{f}{2D}V|V| = 0$$

Choosing $\lambda = -a$ **as the other scale factor permits writing equation (7) as:**

$$\ldots (11)\ \frac{dV}{dt} - \frac{1}{a\rho}\frac{dP}{dt} + g\sin\theta + \frac{f}{2D}V|V| = 0$$

Remember, equation (10) is good only when: $\lambda = +a$ **or** $\frac{ds}{dt} = a$

and equation (11) is good only when : $\lambda = -a$ **or** $\frac{ds}{dt} = -a$

The result of these manipulations is that the two partial differential equations (4) and (5) are replaced by two ordinary differential equations (10) and (11) following certain rules, which relate the independent variables x and t in each case. If in addition, replacing *p* with *γ(H-z)*, Wylie, E.B. and Streeter, V.L. (1993) ,this substitution dives :

$$\ldots (12)\ \frac{dV}{dt} + \frac{g}{a}\frac{dH}{dt} + \frac{fV|V|}{2D} = 0 \qquad \text{only when } \frac{ds}{dt} = a$$

While

$$\ldots (13)\ \frac{dV}{dt} - \frac{g}{a}\frac{dH}{dt} + \frac{fV|V|}{2D} = 0 \qquad \text{only when } \frac{ds}{dt} = -a$$

The fact that the relation between *x* and *t* in equation (12) must satisfy *(ds/dt=a)*, has caused the equation (*ds/dt=a*) which is called the characteristic equation (12). A similar line of reasoning suggests that (*ds/dt=-a*) is the characteristic equation (13).

Fig.(3), which is line *x-t* plane for some unknown problems is examined. It is known that at any point on the *x-t* plane, say point *P*, the value of *H* and *V* is unique (i.e., the *H* and *V* values are independent of which characteristics they are approached from). It is also known that if the *C+* and *C–* characteristics are

constructed through this point, two ordinary differential equations are obtained, which apply along their respective characteristics. The ordinary differential equations can now be expressed in finite difference from equation (12) which becomes:

$$\ldots(14)\ \frac{V_P - V_{Le}}{t_P - 0} + \frac{g}{a}\frac{H_P - H_{Le}}{t_P - 0} + \frac{fV_{Le}|V_{Le}|}{2D} = 0$$

and equation (13) which becomes :

$$\ldots(15)\ \frac{V_P - V_{Ri}}{t_P - 0} - \frac{g}{a}\frac{H_P - H_{Ri}}{t_P - 0} + \frac{fV_{Ri}|V_{Ri}|}{2D} = 0$$

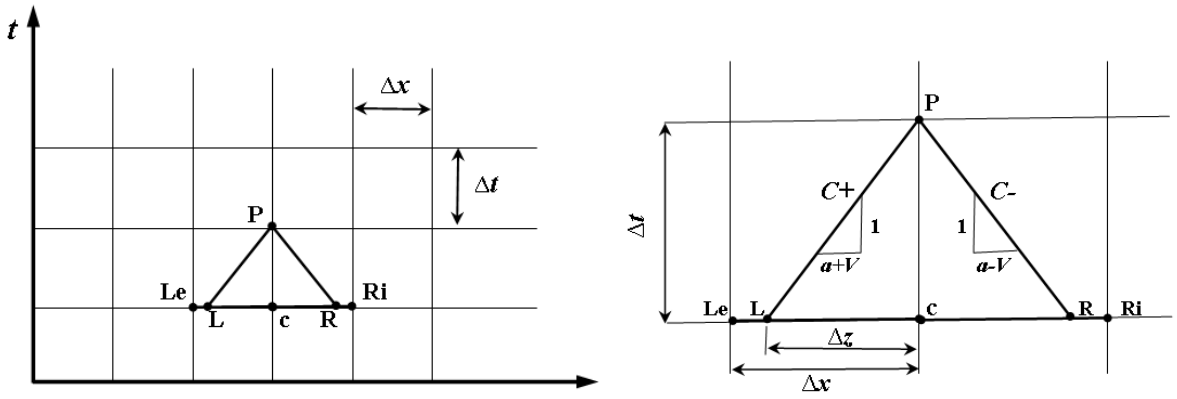

Fig. 3 Interpolation of *H* and *V* values on a Δx-Δt grid.

In the preceding equations, (t_p-*0*) in general is Δt, and when these equations are multiplied by Δt, they become:

$$\ldots(16)\ C^+ : \left(V_P - V_{Le}\right) + \frac{g}{a}\left(H_P - H_{Le}\right) + \frac{f\Delta t}{2D}V_{Le}|V_{Le}| = 0$$

and

$$\ldots(17)\ C^- : \left(V_P - V_{Ri}\right) - \frac{g}{a}\left(H_P - H_{Ri}\right) + \frac{f\Delta t}{2D}V_{Ri}|V_{Ri}| = 0$$

Each of the characteristic equation can be integrated to show that:

$$\ldots(18)\ \Delta x = a\Delta t$$

Once a finite difference numerical solution is used, the pipe must be divided into a discrete number of sections and proceed accordingly. If the pipe is divided into N sections, then each section will be of $\Delta x = L/N$ length. Thus, Δt can be calculated. It is possible to construct a grid of characteristics.

Grid points along the *x*-axis represent points spaced Δx apart along the pipe and the values of *V* and *H* at these points on the *x*-axis represent initial conditions. Initial conditions are, generally, some steady state flow situation in the pipe. Picking a point P_2 in the pipe on the *x*–*t* plane and writing equations (16) and (17)

for the known V_{Le}, V_{Ri}, H_{Le}, H_{Ri}, f and D, it becomes clear that the equation have two unknowns. The two equations can be solved easily for H_{P2} and V_{P2}. Notice that the known velocities are used to represent the friction term. To do otherwise would render the equations difficult to solve and would not noticeably improve the solution except when friction losses are very large. In the exceptional case, an iterative procedure is to be developed wherein friction losses would depend on a velocity averaged in some manner over the time interval.

The procedure described for point P_2 , can be continued for other points until the values of H and V at points P_2 through P_N are calculated. The values of H and V at P_1, P_{N+1} must be calculated with the assistance of boundary conditions. At the left-hand end of the pipe (near $x=0$) only the C^- equation is obtained which relates conditions between x_2 and x_1. The boundary conditions at x_1($x=0$) must provide another equation in H_{P1} and/or V_{P1} to be solved simultaneously with the C^- equation. The same situation and requirements exist at the downstream end of the pipe with the C^+ characteristic.

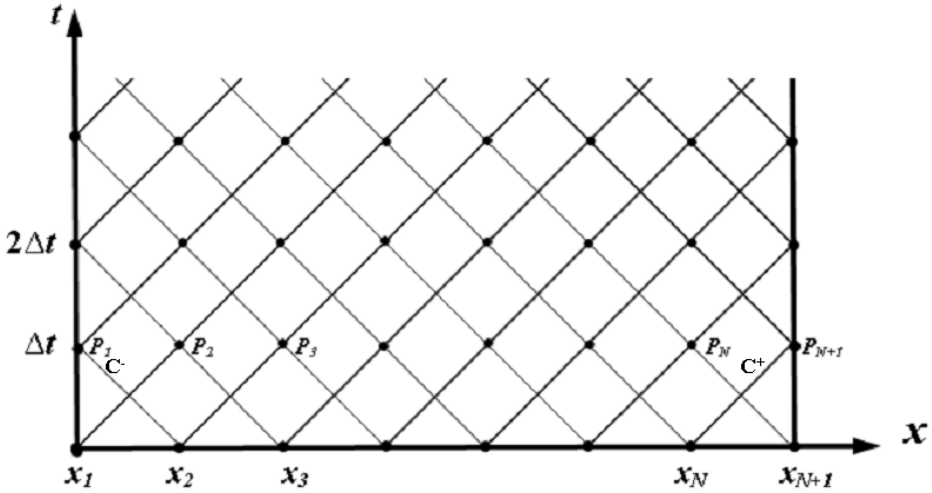

Fig. 4 The method of characteristics staggered grid for a reservoir-pipe-valve system

Once the boundary conditions are established, velocities and total heads at all the grid points at $t=\Delta t$ can be calculated. These values are now used to write new equations to solve the values of V and H at the next time step where $t=2\Delta t$. This procedure is repeated until the solution has progressed the required amount of time. The result is a set of H and V values at discrete time intervals for $N+1$ location along the pipe.

The numerical solution procedure first assumes that the characteristic curves can be approximated as straight lines over each Δt time interval. This assumption appears to be promising because $a>>V$; however. It should be carefully noticed that the slope of each characteristic is generally slightly different from that of any other. The problem created in the finite difference approximation to the differential equations can be seen in Fig.(4). This grid size Δx by Δt has been set and once again the procedure is to find the values of V and H at P. The curved characteristics intersecting at P are approximated by straight lines. The slope of

the straight lines is determined by the known value of velocity at the earlier time. It is important to note that the characteristics passing through *P* do not pass through the grid points *Le* and *Ri*, but pass through the *t*=constant line at points *L* and *R* somewhere in between.

From the completion and modification of equations (16) and (17), the following results:

$$\dots (19)\ \frac{V_P - V_L}{\Delta t} + \frac{g}{a}\frac{H_P - H_L}{\Delta t} - \frac{g}{a}V_L \sin\theta + \frac{f}{2D}V_L|V_L| = 0$$

$$\dots (20)\ \frac{V_P - V_R}{\Delta t} - \frac{g}{a}\frac{H_P - H_R}{\Delta t} + \frac{g}{a}V_R \sin\theta + \frac{f}{2D}V_R|V_R| = 0$$

The values of V_L, H_L, V_R, H_R are not known.

However, the values of V_{Le}, H_{Le}, V_{Ri}, V_C and H_C are known. The unknown value of H and *V* at points *L* and *R* can be estimated by interpolation. In this case, linear interpolation will be used and the sketch below illustrates the relationships.

Considering the C^+ characteristic

$$\frac{\Delta x}{\Delta s} = \frac{V_L - V_C}{V_{Le} - V_C} = \frac{H_L - H_C}{H_{Le} - H_C}$$

Where $\frac{\Delta x}{\Delta t} = \frac{a + V_L}{1}$

Solving of V_L and H_L gives:

$$V_L = (V_{Le} - V_C)\frac{\Delta x}{\Delta s} + V_C$$

and

$$H_L = (H_{Le} - H_C)\frac{\Delta x}{\Delta s} + H_C$$

Substituting the value of $(\Delta x/\Delta t)=a+V_L$ gives:

$$\dots (21)\ V_L = \frac{V_C + a\frac{\Delta t}{\Delta s}(V_{Le} - V_C)}{1 - \frac{\Delta t}{\Delta s}(V_{Le} - V_C)}$$

and

$$\dots (22)\ H_L = H_C + \frac{\Delta t}{\Delta s}(H_{Le} - H_C)(a + V_L)$$

a similar analysis for the C^- characteristic gives:

$$\dots (23)\ V_R = \frac{V_C + a\frac{\Delta t}{\Delta s}(V_{Ri} - V_C)}{1 + \frac{\Delta t}{\Delta s}(V_{Ri} - V_C)}$$

and

$$\ldots (24)\; H_R = H_C + \frac{\Delta t}{\Delta s}(H_{Ri} - H_C)(a + V_R)$$

because ($\Delta t/\Delta s$) V_{Ri}-V_C is of the order $V/(a+V)$ which is very small compared with 1, it is a good approximation to neglect the second terms in the denominators of equations (21) and (23). The result is:

$$\ldots (25) V_L = V_C + a\frac{\Delta t}{\Delta s}(V_{Le} - V_C)$$

and

$$\ldots (26) V_R = V_C + a\frac{\Delta t}{\Delta s}(V_{Ri} - V_C)$$

The simultaneous solution of equations (19) and (20) for V_P and H_P gives:

$$(27) V_P = \frac{1}{2}\left[(V_L + V_R) + \frac{g}{a}(H_L - H_R) + \frac{g}{a}\Delta t(V_L - V_R)\sin\theta - \frac{f\Delta t}{2D}(V_L|V_L| + V_R|V_R|)\right]$$

$$(28) H_P = \frac{1}{2}\left[(H_L + H_R) + \frac{a}{g}(V_L - V_R) + \Delta t(V_L + V_R)\sin\theta - \frac{a}{g}\frac{f\Delta t}{2D}(V_L|V_L| - V_R|V_R|)\right]$$

where $\sin\theta = dz/dx$ (positive for pipes sloping upward and negative in downstream direction)

5. Boundary Conditions

The boundary conditions, corresponding to the valve-pipe-reservoir configuration shown in Fig. 1, and assuming a sudden valve closure, are

At the valve ($x=L$)

$$0 > \ldots (29) V_o(L,t) = 0 \qquad t$$

At the reservoir ($x=o$)

$$0 > \ldots (30)\; p(0,t) - \rho g H + \frac{1}{2}\rho(1 + K_R)V_0^2(0,t) = 0 \qquad t$$

Where K_R is the loss coefficient of the reservoir, and

$$H = \frac{(1+K_R)}{2g}V_{HP}^2 + \frac{8\nu L}{gR^2}V_{HP}$$

Where V_{HP} is the mean velocity of the initial Hagen-Poiseuille flow.
Denotes the height of the fluid in the reservoir, which is considered constant.

6. Case study

In order to show the results of the application of the present work, the experiment carried out by Holmboe, E. L. and Rouleau, W.T. (1967), is reproduced. The

experiment corresponds to the situation shown in Fig. 1, in which the relevant parameters are the following:

Pipe length, L = 36 m, Pipe radius, R = 0.0127 m,

Kinematic viscosity, ν = 39.67 10-6 m²/s (at 27°C), Speed of sound, a = 1324.4 m/s , The initial condition is a fully established Hagen-Poiseuille flow, with the valve completely open. At time t=0, the valve is suddenly closed.

The following values were considered for the loss coefficient of the reservoir, K_R

$$K_R = \begin{cases} 1.0 if V_0(o,t) \geq o \\ 0.5 if V_0(o,t) < o \end{cases}$$

7. Results and Discussion

In Figs. 5 and 7, the time histories of pressures and mean velocities, all of them at x=L/2, are shown in non-dimensional form. Similarly, Figure 6 shows the pressure history at the valve, i.e. at x=L.

It is clear from Figs. 5 to 7 that the quasi-steady model provides a poor representation of the histories of all of the variables considered

Results of the present work are compared against the experimental data of Holmboe, E. L. and Rouleau, W.T. (1967), the numerical model proposed by Zielke W. (1967), Vardy A. and Hwang K. (1991) and that of Prado, A. and Larreteguy, A. (2003).

The note from Fig 5 and 6, the pressure histories that are in good agreement with both experimental, Zielke's numerical results and Prado.

Fig. 7 shows the dramatic difference in the histories of mean velocities obtained with the present model as compared to that obtained with the quasi-steady model.

8. Conclusions

The characteristics method is the most widely used method used to calculate pressure variations in unsteady flow, because, it is a numerical method with the capability of including most of the boundaries. Other methods require more assumptions and simplifications of the boundary conditions and this leads to a reduction in the analysis and results in accuracy. The ability of using of this method in computer programs increases its efficiency, resulting in accuracy and speed of analysis.This approach, as compared to the usual quasi-steady model, allows for a better representation of the pressure and velocity. In fact, the quasi-steady model is a particular case (the simplest and less-accurate one) of the new method.The test of the present work against experimental results by Holmboe and Rouleau, and mathematical models and numerical simulations of other authors, Zielke W. and Prado, A. and Larreteguy, E., show that the present work is able of obtaining comparable results. Moreover, the present methodology results simpler and less memory demanding than that of reference, Prado, A. and Larreteguy, E., which requires the storage of the history of the motion.

The present approach should also be able to deal with turbulent flows, although this would require the identification of a different set of exponents, or even the selection of an expansion other than into a polynomial one. This appears as the natural continuation of the present work.

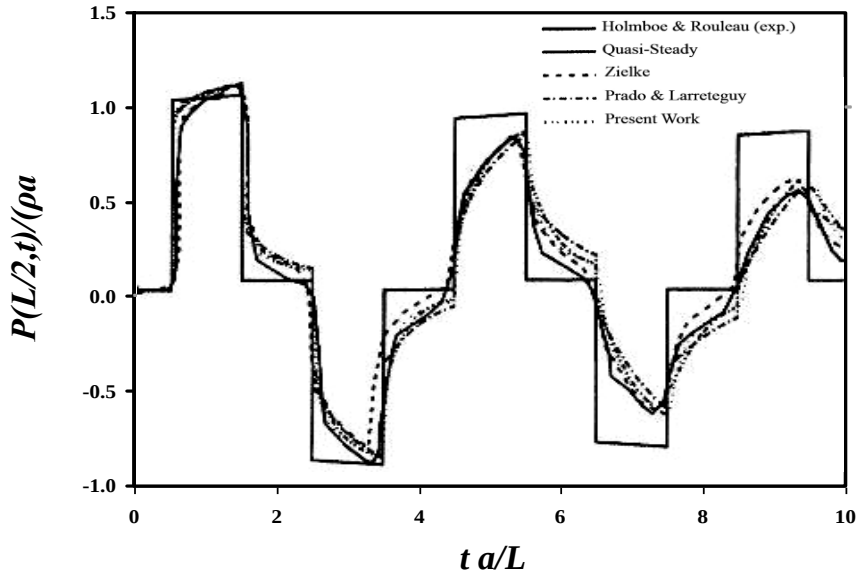

Fig 5 Head fluctuation at midstream (*x=L/2*) after instantaneous valve closure.

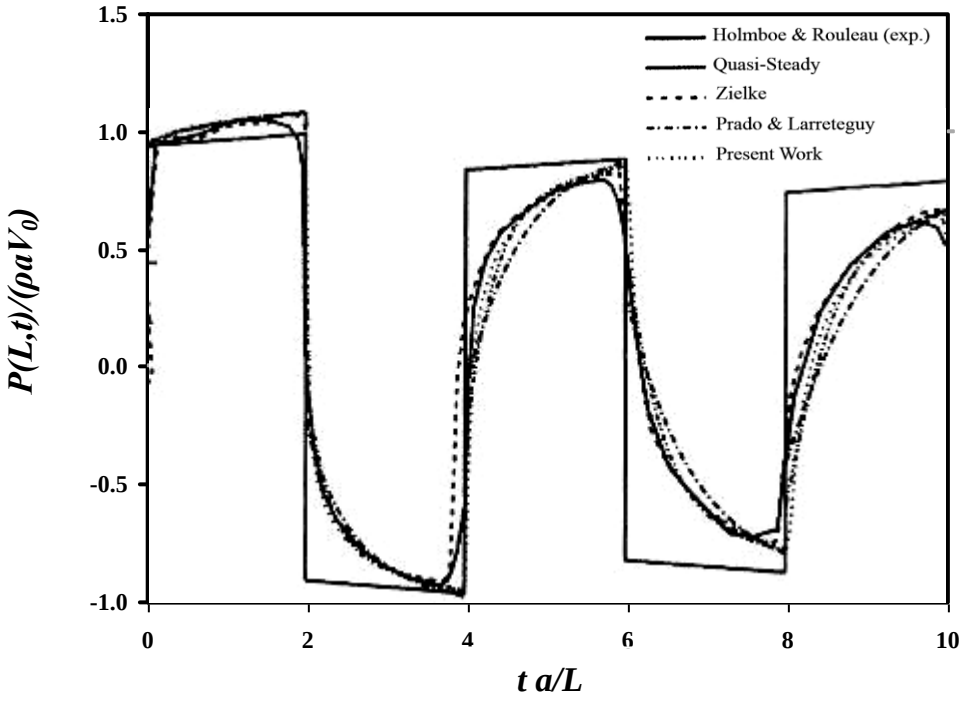

Fig 6 Head fluctuation at valve (*x=L*) after instantaneous valve closure.

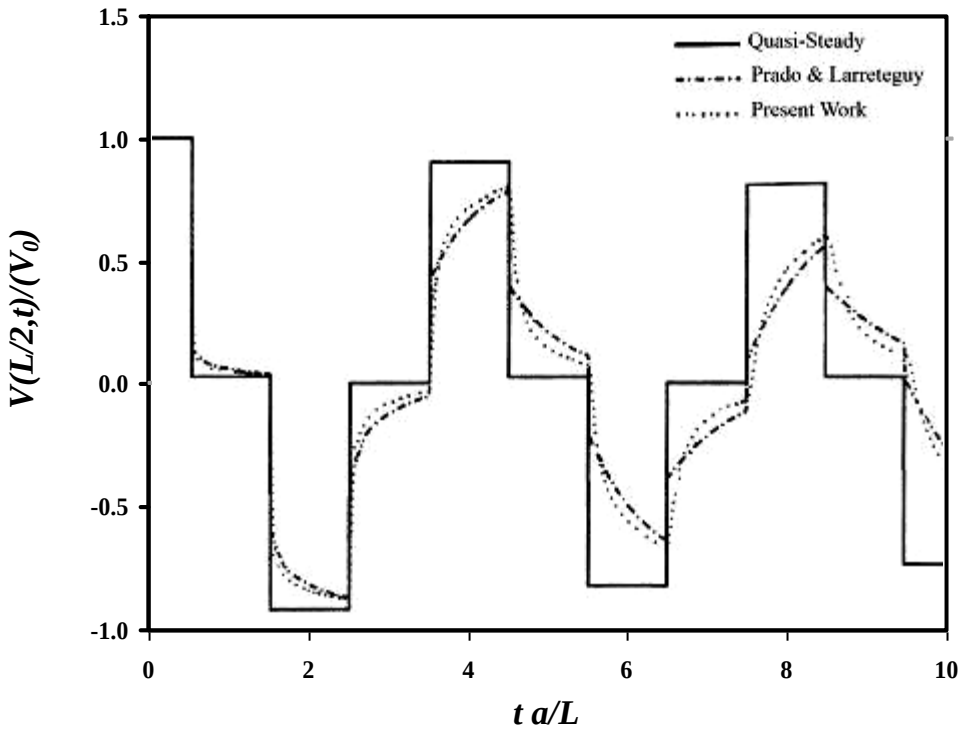

Fig 7 Mean velocity at *x=L/2*

References:

Amein, M. and Chu, H. (1975) ''*Implicit Numerical Modeling of Unsteady Flows*''. J. Hyd. Div. ASCE Vol. 101, No. 6, Pp. 717-731.

Bergant, A., Tijsseling, A., Vítkovský, J., Covas, D., Simpson, A., and Lambert, M. (2005). "*Further Investigation of Parameters Affecting Water Hammer Wave Attenuation, shape and Timing. Part 1: Mathematical Tools*." The Surge-Net project (see http://www.surge-net.info) is supported by funding under the European Commission's Fifth Framework 'Growth' Programme via Thematic Network "Surge-Net" contract reference: G1RT-CT-2002-05069.

Bergant, A., and Tijsseling, A. (2001). "*Parameters Affecting Water Hammer Wave Attenuation, Shape and Timing*." Proceedings of the 10th International Meeting of the IAHR Work Group on the Behaviour of Hydraulic Machinery under Steady Oscillatory Conditions, Trondheim, Norway, Paper C2, 12 pp.

Holmboe, E. L. and Rouleau, W. T. (1967) ''*The Effect of Viscous Shear on Transients in Liquid Lines*''. ASME Journal of Basic Engineering. March. Vol. 89. Pp.174-180.

Prado, A. and Larreteguy, E. (2002). "*A transient Shear Stress Model for the Analysis of Laminar water-Hammer Problems*." Journal of Hydraulic Research, Vol. 40,, No. 1, Pp. 45-53.

Vardy A. and Hwang K. (1991) ''*A characteristics Model of Transient Friction in Pipes*.'' Journal of Hydraulic Research, Vol. 29, No. 5, Pp. 669-683.

Vuuren, S.(2002) ''*Theoretical Overview of Surge Analysis*''. University of Pretoria.

Wylie, E.B. and Streeter, V.L. (1993) ''*Fluid transients in systems*''. Prentice Hall, Englewood Cliffs, ZDA.

Zielke W. (1967) ''*Frequency-Dependent Friction in Transient Pipe Flow*''. Paper No. 67-WA/FE-15.